

# OXBOW EFFECT AND SURFACE TEMPERATURE PROFILES OF CALENDER ROLLS

External heating and proper design are solutions

BY J. ZWART AND W.R. FARRELL



J. Zwart,  
Abitibi-Price  
Inc., Central  
Research, Mis-  
sissauga, Ont.



W.R. Farrell,  
Abitibi-Price  
Inc., Central  
Research, Mis-  
sissauga, Ont.



THE CALENDAR STACK must have a uniform nip gap along its entire width to produce a sheet with uniform CD caliper profile. The CD caliper profile control system can compensate for minor variations but cannot always compensate for the caliper variations at the paper edge caused by the oxbow effect. A typical example is shown in Fig. 1.

There is very little literature published on the oxbow effect and what does exist [1] does not clearly describe the different sources of the oxbow effect and the importance of each source. Only when these sources are clearly understood can the roll designer do a proper job of designing new calendar rolls or developing new concepts for heating calendar rolls.

An improperly designed roll can cause soft reel edges due to the increased roll diameter near the journal ends. Understanding the oxbow effect is also important for the end user to select the optimum roll design and

to gain the maximum performance from his calendar stack.

In this report the sources of the oxbow effect are discussed in a qualitative sense. This information is augmented with examples of finite element results to show the relative importance of each of these effects. In addition, the surface temperature profiles of a number of calendar rolls of various designs were measured under operating condi-

tions. Three types of rolls, all of 610-mm diameter were measured, two displacement body rolls, one with 101.6-mm shell thickness, the other with 152.4-mm shell thickness and a tripass roll with 15 hot water holes.

## OXBOW EFFECT

Typically, the roll is ground to a uniform diameter at room temperature.

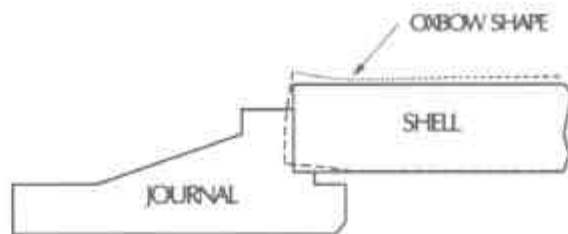


FIG. 1. THE TOP HALF OF THE CROSS SECTION OF A CALENDAR ROLL END SHOWING THE TYPICAL "OXBOW SHAPE".

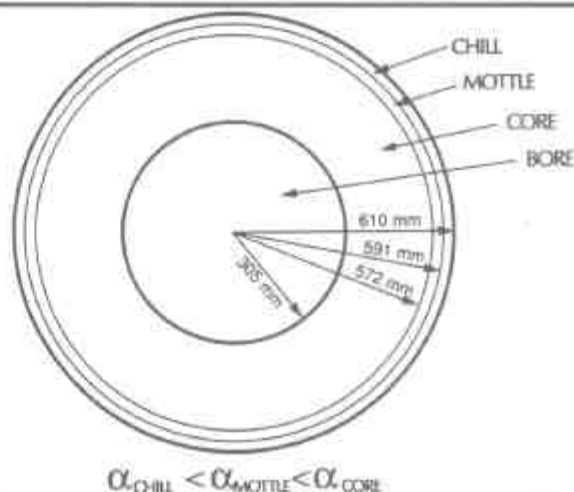


FIG. 2. CROSS-SECTION OF CALENDAR ROLL SHOWING THE LAYERS OF CHILL AND MOTTLE ON THE CORE IRON.

However, under operating temperatures the roll diameter decreases toward the end of the roll and then increases as shown in Fig. 1. This is referred to as the oxbow shape.

The heat flow through the cross-section of the calender roll at its lengthwise midpoint is one-dimensional in the radial direction. Near the journal ends the heat flow becomes two-dimensional. The major direction of heat flow is still in the radial direction but there is also some heat flow in the axial direction.

The distortion causing the oxbow effect has three temperature related sources which are additive. To visualize the first two sources, ignore the end effects noted above, and assume the heat flow is in the radial direction only.

**Source 1: Uniform temperature effects:** Figure 2 shows the construction of a typical straight bore calender roll with a 19-mm layer of chilled cast iron on the outer surface and a 19-mm layer of mottle iron between the chill and core iron. The layer of chill iron has a lower co-efficient of thermal expansion than the mottle and the core iron has the highest value. When the roll is uniformly heated, the surface of the roll is under tension and the core is under compression due to the differing values of thermal expansion.

The boundary conditions on a thin cross-sectional slice at the lengthwise midpoint of the roll are such that the adjacent roll material prevents the stresses developed from causing any non-uniform axial deformation. When the slice is taken from the end of the roll, the restraint provided by adjacent material on the outboard side is no longer present.

With the stresses removed, the interior material can expand axially outward to a much greater extent than the surface material. This is equivalent to putting a large concentric moment on the roll end which causes the roll to grow in diameter at the very end and be reduced in diameter a short distance in from the end, Fig. 1.

**Source 2: Radial temperature gradient effects:** During normal operation, the surface of the roll is heated by the hot water flowing in the bore. Thus, the interior of the roll is hotter than the surface, Fig. 3. The hotter interior temperatures cause similar stresses to those described above, accentuating the distortion.

**Source 3: Actual temperature effects:** Heat flow at the journal end of the roll is not constrained to the radial direction, but also flows in the axial direction resulting in a hotter volume average temperature at the end. Figure 4 shows such a temperature profile where the surface temperature changes rapidly at the roll end. This is caused by the

higher rate of heat flow into the paper in the wrapped portion of the roll, as compared to the heat flow into the air at the unwrapped end of the roll.

Thus the surface temperature at the roll end tends to be hotter than the surface temperature in the wrapped portion of the roll. The amount of expansion at the end is dependent upon the volume average of the temperature rise at the roll end.

In a poorly designed roll, the volume average temperature will be much higher at the end than at the centre causing the roll to have a larger diameter at the end.

## SOURCE CONTRIBUTION

SDRC IDEAS was used to construct a finite element model of a 610-mm diameter displacement body hot water roll, with a 152.4-mm thick shell, to test the relative importance of each of the sources. The calculation was done without the journal to properly simulate radial temperature gradient effects. The absence of the journal ends does affect the structural boundary conditions which will give a higher distortion value.

To simulate the contribution of the uniform temperature effect, the roll was assumed to have been ground to a uniform diameter at 22°C and heated to a uniform temperature of 90°C. The additional contribution of the radial temperature gradient effect was simulated by using 140°C water in the bore with a film co-efficient of 9749 W/(m<sup>2</sup>K).

Finally, the contribution of the actual roll end temperature was simulated by using the surface temperature profile measured on an operating calender stack as the thermal boundary condition at the surface. This temperature profile was measured on a displacement body roll of 152.4-mm shell thickness, Fig. 9.

The increased diameter of the roll due to the thermal effects is shown cumulatively for the three sources in Fig. 5 as a function of the distance from the roll end. There is only a minor contribution due to the effect of the differing thermal expansion values. The major contribution is due to the effects of the radial temperature gradient. The volume average temperature rise does not contribute significantly here either.

Since the radial temperature gradi-

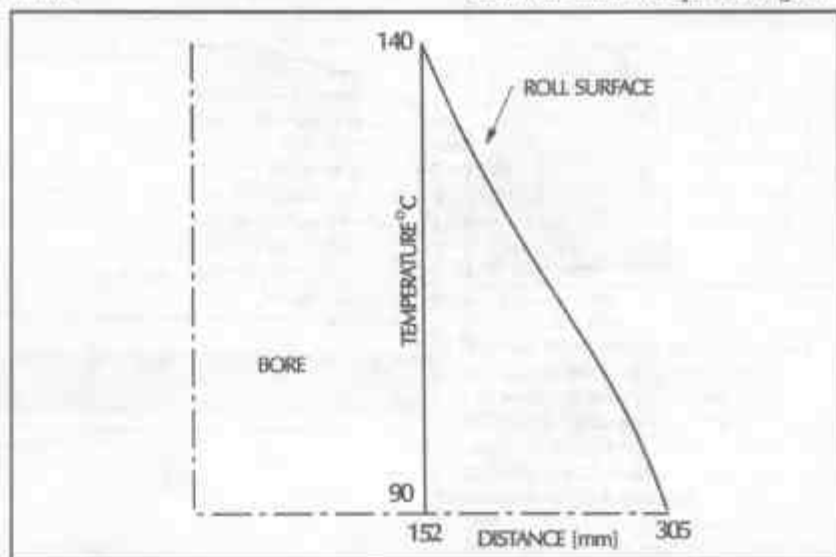


FIG. 3. TEMPERATURE PROFILE THROUGH THE SHELL SHOWING THE HOT INTERIOR AND COOLER SURFACE.

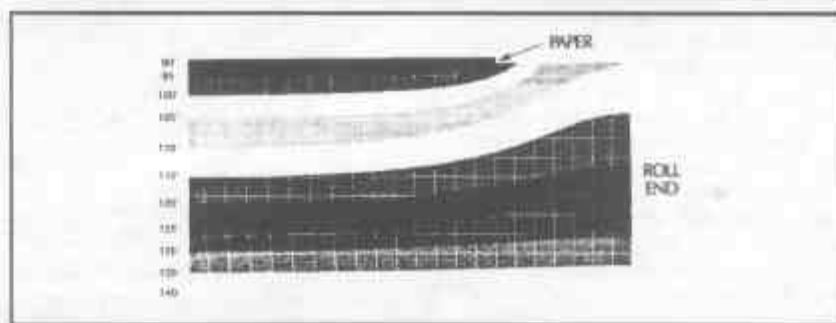


FIG. 4. THE TEMPERATURE PROFILE OF A HOT ROLL END.

ent has the largest contribution to the oxbow effect, the most effective method to reduce oxbow deformation is to minimize the thermal resistance of the calender roll. The relative importance of the roll thermal resistance and the volume average end temperature will be influenced by the absence of the journal.

## 1 THERMAL RESISTANCE

If a calender roll has a low thermal resistance which results in a small temperature drop through the shell, the major contributor to the oxbow effect is reduced. The lower thermal resistance will also reduce the axial heat flow at the roll ends which will reduce the contribution of the actual temperature profile.

Appendix I shows a test case where an estimate of the upper bound of the thermal resistance of the 610-mm tripass roll was calculated and compared to the thermal resistance of 610-mm diameter displacement body rolls with 152.4-mm shell thickness and 101.6-mm shell thickness. The tripass roll has 15 holes of 44.45-mm diameter at 476.25-mm bolt circle diameter.

Using the approximate analytical calculation gives its thermal resistance to be  $1.03 \times 10^{-3} \text{K/W}$  per metre of roll length. This approximation has been checked with a finite element simulation which predicts a thermal resistance of  $0.87 \times 10^{-3} \text{K/W}$  per metre of roll length. The displacement body with the 152.4-mm shell thickness has a thermal resistance of  $3.04 \times 10^{-3} \text{K/W}$  per meter of length and with a 101.6-mm shell thickness has a thermal resistance of  $1.76 \times 10^{-3} \text{K/W}$  per metre length.

Thus, the resistance of the 152.4-mm shell thickness roll is 3.5 times greater than that of the tripass roll and that of the 101.6-mm shell thickness is twice as great.

Since the largest contribution to the oxbow effect is from the radial temper-

ature profile, the best design to minimize the oxbow effect will have the lowest temperature drop across its shell. The tripass roll has the lowest thermal resistance, thus it will also have the lowest temperature drop.

It has the added advantage of having the temperature drop across a small portion of the roll with over half of the material at a uniform temperature. Thus it will have the least tendency to distort.

## 0 OPTIMUM TEMPERATURE

The ideal temperature profile on a calender roll can be described as the profile that gives the most uniform reel. Since the nip load is the most important parameter affecting the web consolidation, the load, or roll diameter within the paper trim, must be as uniform as possible.

Uniformity of the roll surface temperature is the second most important factor as shown in the calendaring equation developed by Crotagino [2].

There are a number of variables involved in the temperature and distortion of the roll ends. They are:

- Roll geometry details;
- Internal roll insulation;
- Temperature of the heating fluid;
- Heat transfer co-efficients between the heating fluid and roll;
- Heat transfer co-efficient between the roll and air;
- Ambient air temperature;
- Sheet temperature;
- Sheet basis weight and moisture;
- Contact resistance between the sheet and roll which are functions of the sheet bulk, tension, and roughness;
- Sheet trim.

These variables indicate the care required in the proper design of a calender roll, and the fact that seemingly insignificant changes such as the machine trim can affect calender performance.

In practice, there cannot be a com-

pletely uniform calender diameter using conventional heating techniques because of the roll's thermal resistance and the large difference in the heat transfer between the wrapped portion of the calender roll and the unwrapped end. The roll can be designed so that the variations are minor. Finite element analysis using SDRC IDEAS was performed to compare the difference between a roll with no end insulation and with insulation installed to minimize heat transfer in the roll end and journal.

The heat transfer co-efficients and temperatures are shown in Fig. 6a and 6b for both cases. The heat transfer co-efficients were calculated from formulae given in Appendix II for a typical 610-mm diameter displacement body roll with a 152.4-mm shell. The temperatures used were measured on an operating calender stack.

The structural boundary conditions are shown in Fig. 6c. The boundary conditions for the roll shell are taken far enough from the roll ends to eliminate any non-uniform axial movement. In the model they are fixed from moving in the axial direction which is shown as axially restrained in Fig. 6c. The model takes the journal end out to about the bearing location. Here the nodes will only move uniformly in the axial direction which is referred to as axially constrained in Fig. 6c.

These calculations give the surface temperature profiles shown in Fig. 7 and the deformations shown in Fig. 8. The uninsulated case shows a definite increase in the roll end diameter which will cause reduced caliper at the paper edges. The insulated case shows that the diameter is smaller at the roll ends. This shows the importance of roll design when internal heating is used.

## M MEASURED TEMPERATURE

A number of calender roll temperature profiles on operating paper

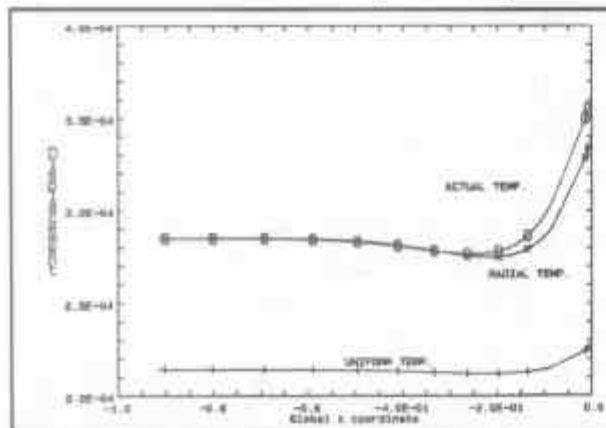


FIG. 5. THE CUMULATIVE ROLL DEFORMATION CAUSED BY THE THREE SOURCES.

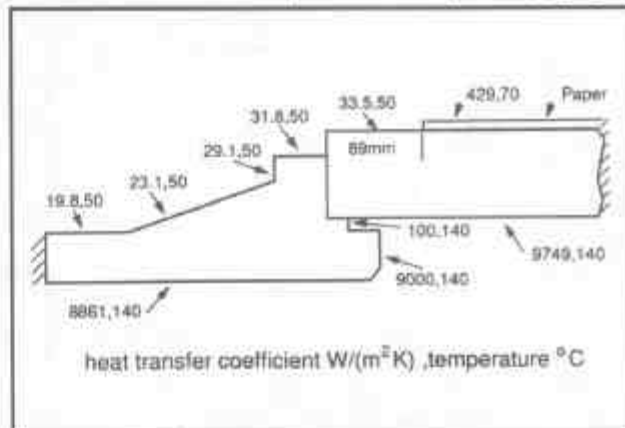


FIG. 6A. THE THERMAL BOUNDARY CONDITIONS FOR AN UNINSULATED JOURNAL.

machines were measured. The temperature measurements on the calender stacks were done with an infrared thermometer. The paper temperature readings were taken directly and an emissivity converter was used to correct for the calender roll surface emissivity. The emissivity converter is quite sensitive to the boundary layer air temperature so care had to be taken near air showers.

The temperatures on a calender roll were taken at three locations outside the paper edge, every 50 to 75 mm inside the paper edge for the first 500 mm, and approximately every 400 to 750 mm in the central portion of the roll. Typical roll end temperature profiles are shown in Fig. 9. The temperature rise at the roll ends roughly correspond to the thermal resistance of the rolls with the tripass being the lowest and the displacement body with the 152.4-mm shell being the highest due to its greater shell thickness.

The temperature profile through a complete stack is shown in Fig. 10. This stack has two heated displacement body rolls with 102.6-mm shells in position 4 and 5 from the bottom, and the remainder of the rolls unheated. The data show the hot roll ends and the

temperature difference between the roll surface and the paper. As expected the unheated rolls do not have hot ends.

## REDUCE OXBOW EFFECT

Four different methods of minimizing the oxbow effect are discussed, along with one method that can be used to anticipate and compensate for the roll deformation before its installation. Some of the methods may not be practical, but the knowledge of their existence will be useful.

**Method 1: Reduce thermal resistance:** The temperature difference between the inside and outside of the roll will be proportionally smaller if it has a lower thermal resistance. This will reduce the oxbow effect by lowering the compressive stress inside the roll and the tensile stress near the surface of the roll. As this has been shown to be one of the major contributors, it is a very important method.

**Method 2: Surface heat the roll:** The most obvious method of surface heating would be to use eddy current heating similar to Calcoils. Surface heating is really an extension of Method 1

where the heat source and sink would both be at the surface of the roll. Thus there would be no contribution to the oxbow effect due to temperature gradients from the interior to the surface of the roll.

This method would also eliminate roll end heating which eliminates its contribution to the oxbow effect. It should be possible to design a roll with controlled end heating or cooling which would compensate for the different thermal expansion co-efficients of the core and chill iron, and thus eliminate the oxbow effect totally.

**Method 3: Hot grind the roll:** With the roll heated to operating temperature on the grinder, the stresses that create the oxbow effect are already present. They are due to the difference in thermal expansion co-efficients in the chill iron versus the core iron. When the roll is ground, this contribution to the oxbow effect is also ground off.

This method, in combination with Method 2, will eliminate all sources of the oxbow effect. However, the contribution to the oxbow effect due to the different thermal expansion co-efficients is minimal, thus hot grinding is not very effective.

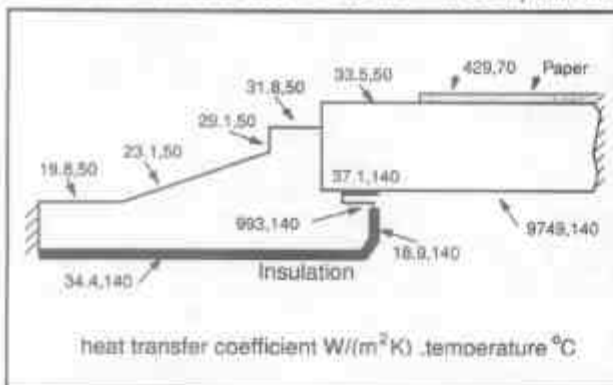


FIG. 6B. THE THERMAL BOUNDARY CONDITIONS FOR THE INSULATED JOURNAL.

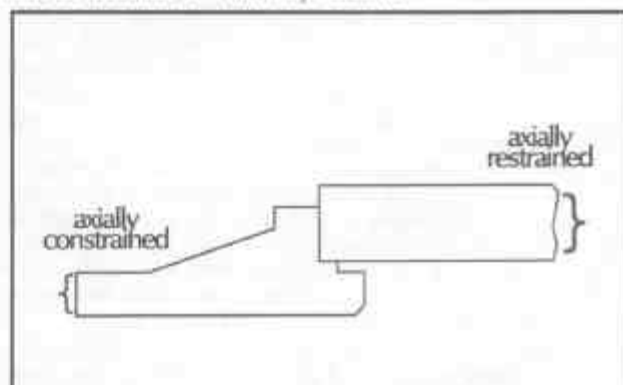


FIG. 6C. THE STRUCTURAL BOUNDARY CONDITIONS.

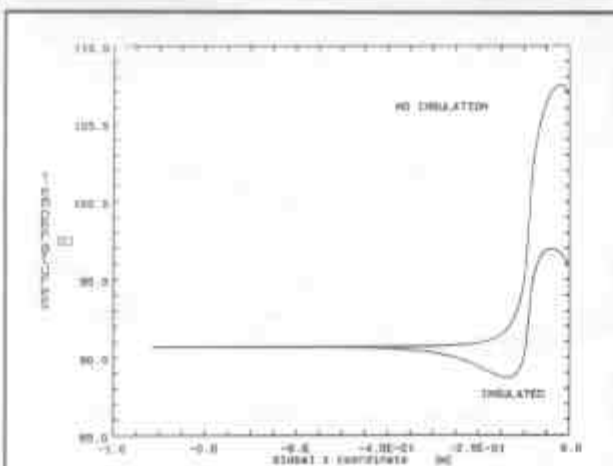


FIG. 7. CALCULATED SHELL END SURFACE TEMPERATURE PROFILES SHOWING THE EFFECT OF INSULATION.

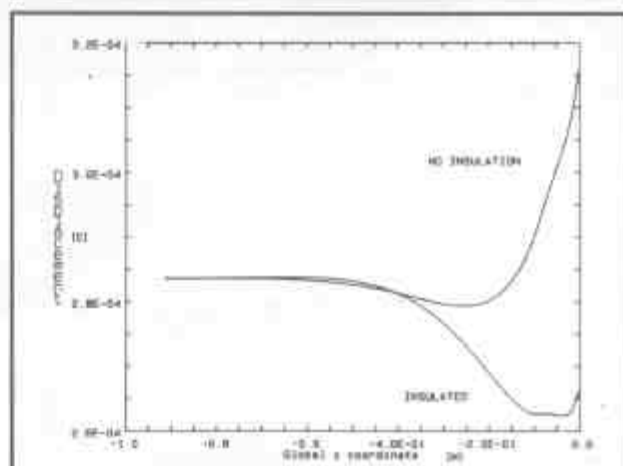


FIG. 8. CALCULATED SHELL END THERMAL GROWTH SHOWING THE EFFECT OF INSULATION.



**Method 4: Compensate using grinder:** In its simplest form the end of a roll is dubbed by an appropriate amount to relieve sheet pinching. This method is usually adequate but can be refined if required. The cold ground shape of the roll can be calculated in such a way that the oxbow effect would straighten the roll under operating conditions. A numerically controlled grinder is envisioned to produce the exact shape required on the cold roll for a given set of operating conditions.

**Method 5: Use a well-designed roll:** If the manufacturer knows the exact operating parameters of the calender, and the required heat transfer co-efficients, he can design the end of the roll to minimize the temperature rise. Ideally, the design band should be wide enough to allow for the normal operating conditions in that particular calender stack. The designer can direct the internal fluid flow correctly, and judi-

ciously place insulation in appropriate locations to minimize heating of the roll ends.

## CONCLUSIONS

The best design of a calender roll using conventional heating from a thermal and distortion point of view is one that has the least thermal resistance. In this respect the tripass roll is clearly the best performer, having a lower thermal resistance than any other calender roll. Internal induction heated calender rolls have similar thermal resistance to that of displacement body rolls. They make the same contribution to the oxbow effect from the radial temperature gradient.

To minimize deformation, the best method of heating a calender roll is by surface heating. This eliminates the contributions to the oxbow effect from hot roll interiors and hot roll ends and

may even be used to compensate for the low co-efficient of thermal expansion on the roll surface. It has the added potential advantage of being able to incorporate caliper profile correction within the system. The roll design would be simplified since it would not have to incorporate the heating passages of the conventional rolls but the total calender design would be bulkier due to the external heaters required for surface heating.

All designs of rolls under most of the operating conditions encountered in this survey had some degree of end heating. The magnitude of the end heating varied with the operating conditions and roll construction; 15°C difference was not uncommon. If roll diameter could have been measured it would have been found that all the rolls had some degree of the oxbow effect. If the increase in roll diameter associated with this effect is outside the edge of

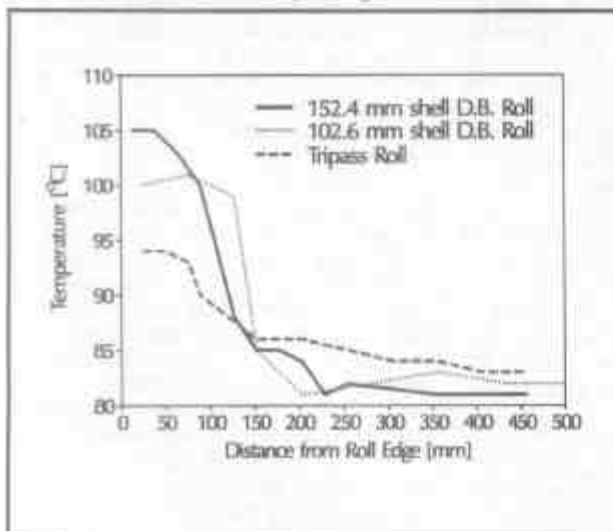


FIG. 9. END TEMPERATURE PROFILES MEASURED ON THE SURFACE OF THREE DIFFERENT TYPES OF CALENDER ROLLS.

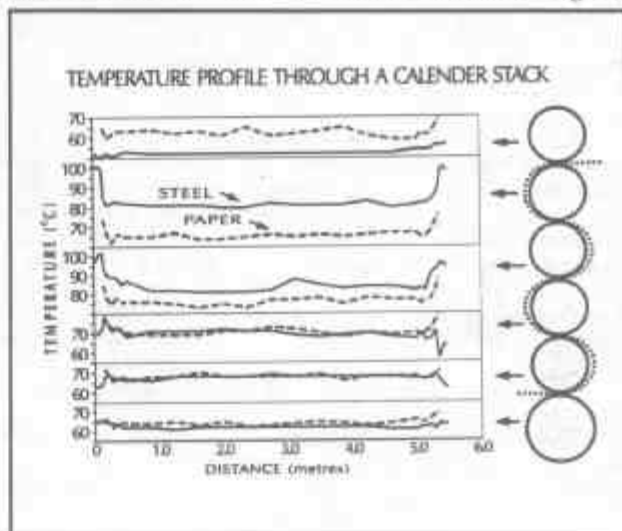


FIG. 10. THE TEMPERATURE PROFILE THROUGH A COMPLETE CALENDER STACK.

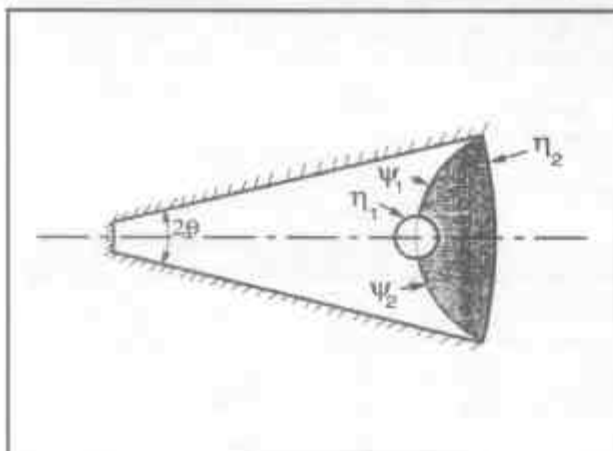


FIG. 11. DIAGRAM SHOWING THE BICYLINDRICAL CO-ORDINATES USED TO CALCULATE THE THERMAL RESISTANCE OF A TRIPASS ROLL.

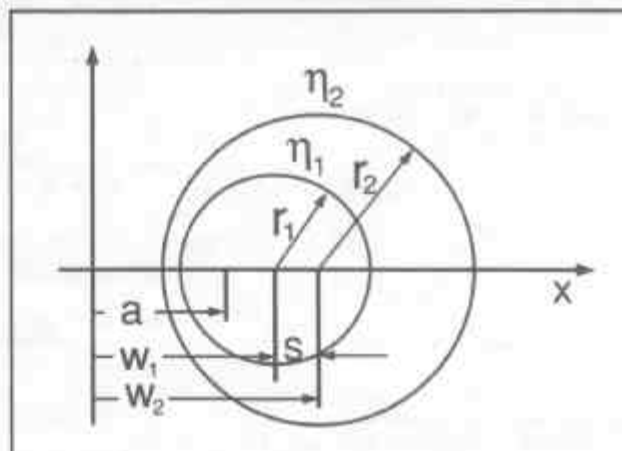


FIG. 12. DIAGRAM SHOWING THE PARAMETERS NEEDED IN BICYLINDRICAL CO-ORDINATES.

the paper, it will have no effect on the paper quality.

Finally, before rolls are purchased by a mill, it should be ascertained that the designer has taken their particular operating conditions into consideration. Designing the roll to minimize the problems associated with the oxbow effect is essential.

## ACKNOWLEDGEMENTS

Special thanks to R. Smith, Valmet-Dominion, for introducing us to the finer details of this subject.

## APPENDIX 1

### Thermal resistance calculations

*Tripass rolls:* Since there is no shape factor readily available to calculate the thermal resistance of a tripass roll an expression is derived. Using symmetry, the roll can be divided into pie shaped sections with one tripass bore hole per section as shown in Fig. 11. The majority of the heat flow is through the section of the bore hole that is closest to the roll surface. Bicylindrical co-ordinates can be used to solve for the heat flow if we assume that all the heat flow occurs in the region bounded by  $\eta_1$ ,  $\eta_2$ ,  $\psi_1$ , and  $\psi_2$ . This gives a high estimate for the thermal resistance since the remainder of the bore hole transmits heat energy as well. The upper bound of the dimensionless thermal resistance in bicylindrical co-ordinates of this segment is given by Yovanovich [3] as:

$$RkL = (\eta_1 - \eta_2) / (\psi_1 - \psi_2) \quad (1)$$

and the remainder of the parameters on the right hand side of the equation are defined as:

$$\eta_i = \sinh^{-1} \{ (w_i/r_i)^2 - 1 \}^{1/2}, i=1,2 \quad (2)$$

$$\psi_1 = \cos^{-1} \{ \cosh(\eta_2) - (a/x) \sinh(\eta_2) \} \quad (3)$$

$$\psi_2 = 2\pi - \psi_1 \quad (4)$$

The remainder of the parameters are given by the following relationships with the aid of Fig. 12:

$$w_1 = (r_2^2 - r_1^2 - s^2) / (2s) \quad (5)$$

$$w_2 = (r_2^2 - r_1^2 + s^2) / (2s) \quad (6)$$

$$a^2 = w_1^2 - r_1^2 = w_2^2 - r_2^2 \quad (7)$$

$$x = w_2 + r_2 \cos(\pi - \theta) \quad (8)$$

For the dimensions given in the text,  $RkL = 0.561$ . With a uniform thermal conductivity of  $36.3 \text{ W/(mK)}$ , and 15 segments in parallel, the resistance is  $1.03 \times 10^{-5} \text{ K/W}$  per metre roll length. This approximate solution was checked using finite element analysis which gave

the thermal resistance as  $0.87 \times 10^{-5} \text{ K/W}$  per metre roll length. Thus the approximate solution is high by 18%.

*Displacement body rolls:* The dimensionless thermal resistance for displacement body rolls is available in standard handbooks [4] as:

$$RkL = \ln(r_o/r_i) / (2\pi) \quad (9)$$

For a 610-mm diameter roll with a 152.4-mm shell thickness, the thermal resistance is  $3.04 \times 10^{-5} \text{ K/W}$  per metre roll length. If instead the roll has a 101.6-mm shell thickness, the thermal resistance is almost half at  $1.76 \times 10^{-5} \text{ K/W}$ .

## APPENDIX 2

### Boundary condition calculations

Accurate material properties and boundary conditions are required to create a model of the calender roll end. The calender roll is constructed so that the outer surface is cooled rapidly to make it very hard. Thus the roll can be considered to have three different materials, Fig. 2. The core, mottle, and chill iron have the thermal and structural properties as shown in Table I. The chill and mottle layers were each assumed to be 19 mm thick.

The temperature distribution in the calender roll needs to be calculated before the resulting structural deformation can be calculated. Thus the thermal boundary conditions also need to be accurately specified. McAdams [5] gives the heat transfer co-efficient for heat flowing outward in an annulus as:

$$(h/(c_p G)) Pr^{2/3} (\mu_s/\mu)^{0.14} = 0.023 / (Re)^{0.2} \quad (10)$$

which is used for the heat flow into a displacement body roll. In this equation,  $h$  is the convective film co-efficient to be solved. Reynolds number uses the hydraulic radius, which is four times the cross sectional area divided by the total wetted perimeter. This value can be verified by tables in the *Handbook for Heat Transfer* [4]. McAdams [5] gives the film co-efficient in a pipe, which is used in the journal bore and tripass rolls, to be:

$$Nu = 0.023 Re^{0.8} Pr^{0.4} \quad (11)$$

where  $Nu$  is the Nusselt number from which the convective film co-efficient can be calculated. The heat transfer from the roll ends to the surrounding air is given by Fechner [6] as:

$$Nu = 0.0226 (Re)^{0.8} \quad (12)$$

The length scale and velocity used in Reynolds number are the local diameter and the surface velocity of the roll.

The final heat transfer co-efficient needed is that of the wrapped portion of the roll. Since only one half of the circumference of the roll is wrapped, the heat can flow from the roll to the air, or from the roll to the paper wrapping it, and also from the roll to the paper in the nip.

Kerekes [7] has shown that the heat transfer to the air is small compared to the heat flow to the paper. Powell and Strong [8] quote a value of  $284 \text{ W/(m}^2\text{K)}$  for the heat flow from dryers to paper with moisture levels similar to that in a calender stack. Kerekes [7] has shown that 33% of the heat flow occurs in the nip if two rolls of uniform temperature are used, which would predict a value of  $424 \text{ W/(m}^2\text{K)}$  on the wrapped portion of the roll.

Burnside and Crocogino [9] measured the heat transfer on a wrapped calender roll with no nip as a function of the paper bulk. This was correlated in two ways: As a contact resistance and paper thermal conductivity; and combined as an effective thermal conductivity. The effective contact resistance between the surface of the calender roll and the side of the paper away from the calender roll is what is required here.

This includes the actual contact resistance and the paper conductivity. It can be obtained from the effective conductivity quoted as  $k_a = 0.069 - 0.0085(\text{bulk})$  where bulk is given in  $\text{cm}^3/\text{g}$  and  $k_a$  in  $\text{W/(mK)}$ . This can be rewritten in terms of an effective contact conductance as  $h_p = k_a/t$  where  $t$  is the paper thickness. Then the film co-efficient for the wrapped portion of the roll is given by:

$$h_p = (0.069 - 0.0085(\text{bulk})) / t \quad (13)$$

with units of  $\text{W/(m}^2\text{K)}$  when  $t$  has units

TABLE I. THE STRUCTURAL AND THERMAL PROPERTIES OF A CALENDER ROLL.

Material properties	Chill	Mottle	Core	Steel journal
Young's modulus (GPa)	172	131	103	207
Poisson's ratio	0.27	0.27	0.27	0.3
Mass density (kg/m <sup>3</sup> )	7694	7583	7334	7835
Co-efficient of thermal expansion (10 <sup>-6</sup> /K)	9.0	9.9	10.8	11.16
Thermal conductivity [W/(mK)]	20.76	31.15	45.68	48.17
Specific heat [J/(kgK)]	586.6	544.6	502.8	628.5

of meters. The temperature difference used across this film co-efficient is the temperature between the outside surface of the calender roll and the temperature measured on the outside surface of the paper. Using typical bulk and caliper values for uncalendered newsprint of 48.8 g/m<sup>2</sup> basis weight and caliper of 150  $\mu$ m gives a film co-efficient of 286 W/(m<sup>2</sup>K). Using the same nip correction factor of 33% cited previously gives the film co-efficient as 429 W/(m<sup>2</sup>K), very similar to the value used by Powell & Strong [8] for the wrapped portion of the roll.

These heat transfer co-efficients are only valid for the wrapped portion of the calender roll. In practice only half of the roll is wrapped, thus the heat transfer co-efficient for the model would be half of the values listed here. Thus the heat transfer co-efficient would be slightly higher than 200 W/(m<sup>2</sup>K) for uncalendered paper.

As the paper is calendered and the bulk is decreased, equation 12 shows that the film co-efficient increases, if the web tension is held constant. The web tension that was used to obtain this relationship [9] was not reported.

Based on observations of bagging in the lower nips of highly loaded calender stacks, the paper tension actually decreases as it goes through a calender stack. This tension reduction will decrease the film co-efficient so it may be reasonable to assume that the heat transfer will not decrease in proportion to the caliper reduction.

The final parameter to be evaluated is the thermal contact resistance between the shell and the journal. This was not done for the analysis reported here but the information for the contact resistance of turned surfaces can be obtained from Yovanovich [10].

## NOMENCLATURE

a - parameter on Fig. 12  
 bulk - inverse of paper density [cm<sup>3</sup>/g]  
 c<sub>p</sub> - specific heat at constant pressure  
 D - diameter for pipes, or  
 4(cross-sectional area)/(total wetted perimeter)  
 G - mass velocity ( $\rho U$ )  
 h - convective film co-efficient  
 k - thermal conductivity  
 K - temperature [Kelvin]  
 L - roll length

Nu - Nusselt No. ( $hD/k$ )  
 Pr - Prandtl No. ( $\mu c_p/k$ )  
 R - thermal resistance  
 Re - Reynolds No. ( $UD/\nu$ )  
 r - circle radius  
 s - parameter from Fig. 12  
 t - paper thickness  
 T - temperature  
 U - mean flow velocity  
 w - parameter from equation 5 and 6  
 x - parameter from equation 7  
 $\alpha$  - co-efficient of thermal expansion  
 $\eta$  - co-ordinates in bicylindrical coordinate system  
 $\mu$  - dynamic viscosity  
 $\nu$  - kinematic viscosity ( $\mu/\rho$ )  
 $\rho$  - density  
 $\theta$  - angle for each tripass segment  
 $\pi$  - pie, 3.141592...  
 $\Psi$  - orthogonal coordinates to  $\eta$   
**Subscripts:**  
 1,2 - for two similar parameters or coordinates  
 a - apparent  
 i - inside  
 o - outside  
 p - paper  
 s - at surface temperature

## REFERENCES

- ROTHENBACHER, P. What's New in Balancing Methods for Chilled Cast Iron Rolls. *PAMA* 32-37 April 1988.
- CROTOGINO, R.H., HUSSAIN, S.M. McDONALD, J.D. Mill Application of the Calendering Equation. *JPPS* Nov. 1985 (TR128-154).
- YOVANOVICH, M. M. Advanced Heat Conduction. MEGI Advanced Heat Conduction Course Textbook available from the Author through the University of Waterloo, Waterloo, Ontario.
- KOHSENOW, W. H. HARTNETT, J. P. Handbook of Heat Transfer. New York: McGraw-Hill Book Company, 1984.
- McADAMS, W. H. Heat Transmission. New York: McGraw-Hill Book Company 1954.
- FECHNER, G. Waermeuebertragung bei senkrecht auftreffenden Strahl an der Platte und an Rohr. Dissertation T.V., Muenchen 1971.
- KEREKES, R. J. Heat Transfer in Calendering. Trans. Tech. Sec. Vol. 3(3) TR 66-76 Sept. 1979.
- POWELL, T., STRONG, A. B. An Analysis of Drying on Conventional Paper Machines. *Pulp Paper Mag. Can.* 75 (3):T77 (March 1974).
- BURNSIDE, J. R., CROTOGINO, R. H. Some Thermal Properties of Newsprint and Their Variations with Bulk. *JPPS* Vol. 10, No. 6, J144-J150, Nov. 1984.
- YOVANOVICH, M. M. Thermal Contact Conductance of Turned Surfaces. Paper 71-80 at the 9th Aerospace Sciences Meeting, New York, N.Y., Jan 25-27, 1971.

**Résumé:** Nous nous sommes servis de l'analyse des éléments finis pour calculer les profils de la température et de la distorsion thermique à l'extrémité du rouleau de calendrage. Nous avons comparé les profils de température ainsi calculés avec les profils de température mesurés à la surface du rouleau. Les caractéristiques de fabrication et d'exploitation qui contribuent à la création de l'effet de collier sont le plus faible coefficient de dilatation thermique dans la couche de métal trempé à la surface du rouleau, la température interne plus élevée du rouleau et la température à l'extrémité du rouleau. Pour minimiser l'effet de collier, on fait appel à des techniques qui réduisent la résistance thermique, le chauffage de la surface, le meulage à chaud, le meulage destiné à prévoir et corriger les effets thermiques et à garantir des fabrication thermiquement adaptées.

**Abstract:** Finite element analysis was used to calculate the temperature and thermal distortion profiles at the end of a calender roll. The calculated temperature profiles were compared with the measured temperature profiles on the roll surface. Details of roll construction and operation that contribute to the oxbow effect are a lower co-efficient of thermal expansion in the layer of chill at the surface of the roll, hotter interior roll temperature, and hotter roll end temperature. Techniques that minimize the oxbow effect are reducing thermal resistance, surface heating, hot grinding, grinding to anticipate and correct for the thermal distortions, and ensuring thermally-correct design.

**Reference:** ZWART, J., FARRELL, W.R. Oxbow effect and surface temperature profiles of calender rolls. *Pulp Paper Can* 93(2):T41-47 (Feb. 1992). Paper presented at the 1989 Newsprint Conference of the Technical Section, CPPA, at Quebec, Que., on September 26 to 28, 1989. Not to be reproduced without permission. Manuscript received August 19, 1989. Approved by the Review Panel, June 27, 1990.

**Keywords:** CALENDER ROLLS, THERMAL EXPANSION, TEMPERATURE, PROFILES, DEFORMATION, MATHEMATICAL MODELS, HEAT TRANSFER, PARAMETERS, METHODS ENGINEERING, MACHINE DESIGN.

of meters. The temperature difference used across this film co-efficient is the temperature between the outside surface of the calender roll and the temperature measured on the outside surface of the paper. Using typical bulk and caliper values for uncalendered newsprint of 48.8 g/m<sup>2</sup> basis weight and caliper of 150  $\mu$ m gives a film co-efficient of 286 W/(m<sup>2</sup>K). Using the same nip correction factor of 33% cited previously gives the film co-efficient as 429 W/(m<sup>2</sup>K), very similar to the value used by Powell & Strong [8] for the wrapped portion of the roll.

These heat transfer co-efficients are only valid for the wrapped portion of the calender roll. In practice only half of the roll is wrapped, thus the heat transfer co-efficient for the model would be half of the values listed here. Thus the heat transfer co-efficient would be slightly higher than 200 W/(m<sup>2</sup>K) for uncalendered paper.

As the paper is calendered and the bulk is decreased, equation 12 shows that the film co-efficient increases, if the web tension is held constant. The web tension that was used to obtain this relationship [9] was not reported.

Based on observations of bagging in the lower nips of highly loaded calender stacks, the paper tension actually decreases as it goes through a calender stack. This tension reduction will decrease the film co-efficient so it may be reasonable to assume that the heat transfer will not decrease in proportion to the caliper reduction.

The final parameter to be evaluated is the thermal contact resistance between the shell and the journal. This was not done for the analysis reported here but the information for the contact resistance of turned surfaces can be obtained from Yovanovich [10].

## NOMENCLATURE

a - parameter on Fig. 12  
 bulk - inverse of paper density [cm<sup>3</sup>/g]  
 c<sub>p</sub> - specific heat at constant pressure  
 D - diameter for pipes, or  
 4(cross-sectional area)/(total wetted perimeter)  
 G - mass velocity ( $\rho U$ )  
 h - convective film co-efficient  
 k - thermal conductivity  
 K - temperature [Kelvin]  
 L - roll length

Nu - Nusselt No. ( $hD/k$ )  
 Pr - Prandtl No. ( $\mu c_p/k$ )  
 R - thermal resistance  
 Re - Reynolds No. ( $UD/\nu$ )  
 r - circle radius  
 s - parameter from Fig. 12  
 t - paper thickness  
 T - temperature  
 U - mean flow velocity  
 w - parameter from equation 5 and 6  
 x - parameter from equation 7  
 $\alpha$  - co-efficient of thermal expansion  
 $\eta$  - co-ordinates in bicylindrical coordinate system  
 $\mu$  - dynamic viscosity  
 $\nu$  - kinematic viscosity ( $\mu/\rho$ )  
 $\rho$  - density  
 $\theta$  - angle for each tripass segment  
 $\pi$  - pie, 3.141592...  
 $\psi$  - orthogonal coordinates to  $\eta$   
**Subscripts:**  
 1,2 - for two similar parameters or coordinates  
 a - apparent  
 i - inside  
 o - outside  
 p - paper  
 s - at surface temperature

## REFERENCES

1. ROTHENBACHER, P. What's New in Balancing Methods for Chilled Cast Iron Rolls. *PPMA* 32-37 April 1988.
2. CROTOGINO, R.H., HUSSAIN, S.M. McDONALD, J.D. Mill Application of the Calendering Equation. *JPPS* Nov. 1985 (TR128-134).
3. YOVANOVICH, M. M. Advanced Heat Conduction. MEGI Advanced Heat Conduction Course Textbook available from the Author through the University of Waterloo, Waterloo, Ontario.
4. ROHSENOW, W. H. HARTNETT, J. P. Handbook of Heat Transfer. New York: McGraw-Hill Book Company, 1984.
5. McADAMS, W. H. Heat Transmission. New York: McGraw-Hill Book Company 1954.
6. FECHNER, G. Waermeuebertragung bei senkrecht auftreffendem Strahl an der Platte und an Rohr. Dissertation T.V., Muenchen 1971.
7. KEREKES, R. J. Heat Transfer in Calendering. Trans. Tech. Sec. Vol. 3(3) TR 66-76 Sept. 1979.
8. POWELL, T., STRONG, A. B. An Analysis of Drying on Conventional Paper Machines. *Pulp Paper Mag. Can.* 75 (3):T77 (March 1974).
9. BURNSIDE, J. R., CROTOGINO, R. H. Some Thermal Properties of Newsprint and Their Variations with Bulk. *JPPS* Vol. 10, No. 6, J144-J150, Nov. 1984.
10. YOVANOVICH, M. M. Thermal Contact Conductance of Turned Surfaces. Paper 71-80 at the 9th Aerospace Sciences Meeting, New York, N.Y., Jan 25-27, 1971.

**Résumé:** Nous nous sommes servis de l'analyse des éléments finis pour calculer les profils de la température et de la distorsion thermique à l'extrémité du rouleau de calandre. Nous avons comparé les profils de température ainsi calculés avec les profils de température mesurés à la surface du rouleau. Les caractéristiques de fabrication et d'exploitation qui contribuent à la création de l'effet de collier sont le plus faible coefficient de dilatation thermique dans la couche de métal trempé à la surface du rouleau, la température interne plus élevée du rouleau et la température à l'extrémité du rouleau. Pour minimiser l'effet de collier, on fait appel à des techniques qui réduisent la résistance thermique, le chauffage de la surface, le meulage à chaud, le meulage destiné à prévoir et corriger les effets thermiques et à garantir des fabrications thermiquement adaptées.

**Abstract:** Finite element analysis was used to calculate the temperature and thermal distortion profiles at the end of a calender roll. The calculated temperature profiles were compared with the measured temperature profiles on the roll surface. Details of roll construction and operation that contribute to the oxbow effect are a lower co-efficient of thermal expansion in the layer of chill at the surface of the roll, hotter interior roll temperature, and hotter roll end temperature. Techniques that minimize the oxbow effect are reducing thermal resistance, surface heating, hot grinding, grinding to anticipate and correct for the thermal distortions, and ensuring thermally-correct design.

**Reference:** ZWART, J., FARRELL, W.R. Oxbow effect and surface temperature profiles of calender rolls. *Pulp Paper Can* 93(2):T41-47 (Feb. 1992). Paper presented at the 1989 Newsprint Conference of the Technical Section, CPPA, at Quebec, Que., on September 26 to 28, 1989. Not to be reproduced without permission. Manuscript received August 19, 1989. Approved by the Review Panel, June 27, 1990.

**Keywords:** CALENDER ROLLS, THERMAL EXPANSION, TEMPERATURE, PROFILES, DEFORMATION, MATHEMATICAL MODELS, HEAT TRANSFER, PARAMETERS, METHODS ENGINEERING, MACHINE DESIGN.